Recent and future developments in finite element metal forming simulation

Jean-Loup Chenot, Marc Bernacki, Pierre-Olivier Bouchard, Lionel Fourment, Elie Hachem, Etienne Perchat

Recent and future developments in finite element metal forming simulation

J.-L. Chenot[a,b]*, M. Bernacki[b], P-O Bouchard[b], L. Fourment[b], E. Hachem[b], E. Perchat[a]

[a]*Transvalor, 694 Avenue du Dr. Maurice Donat, 06255 Mougins Cedex, France*
[b]*CEMEF, Mines Paristech, B.P. 207, 06904 Sophia Antipolis Cedex, France*

Abstract

After more than 40 years of development, finite element metal forming simulation has reached a high level of maturity. After a short mechanical and thermal introduction, the main scientific and technical developments are briefly described. We consider numerical issues, such as adaptive remeshing or parallel computing; coupling phenomena for a more realistic simulation, such as thermal and metallurgical coupling, with a special emphasis on modeling of microstructure evolution; the use of optimization for forming processes or for parameters identification. Finally the main potential future research fields for the next 10 years are outlined: process stability and stochastic approaches, more effective massively parallel computing and extension of the application to generate the whole "virtual factory".

Keywords: Plasticity, finite element modeling, metal forming simulation.

1. Introduction

Finite element simulation of metal forming processes started at the end of the sixties, mainly in academic laboratories for 2D work-pieces: hydrostatic extrusion by Iwata et al, hot rolling by Cornfield and Johnson, analysis of relative slip on the tools by Lee and Kobayashi, and large deformations of viscoplastic materials by Zienkiewicz and Godbole. In the 1980's the use of simulation codes started for industrial forming applications, while 3D forging was developed in laboratories by Surdon and Chenot. Since these early developments, commercial finite element computer codes are developed and maintained in several software companies (Transvalor, SFTC, Simufact Engineering GmbH, Quantorform, etc.) which favor their diffusion in large and medium enterprises. Simulation is widely utilized by the engineers as more complex processes can be treated with

a realistic approach. As an example, we can list the availability of the main developments in Forge®, a 3-D commercial code, as follows:

- 1995: automatic remeshing,
- 1996: element quality control,
- 1997: parallel computing,
- 2002: heat treatment, quenching,
- 2003: deformable tools,
- 2005: coupling with metallurgy,
- 2007: thermal regime in tools, multi body forming,
- 2009: "automatic" process optimization,
- 2014: three-dimensional modeling of induction heating.

The main purpose of the paper is to review and analyze the present state of the numerical and physical approaches for treating a wide range of metal forming problems, and discuss briefly new challenges that are emerging.

2. Mechanical and thermal formulations

For a more complete introduction to numerical simulation of metal forming see Wagoner and Chenot.

2.1. Updated lagrangian, eulerian or ALE

The mechanical equations are generally expressed with an integral formulation in term of density ρ, acceleration γ, virtual velocity v*, stress tensor σ, strain rate $\dot{\varepsilon}^*$ and stress boundary condition τ, on the current configuration Ω:

$$\int_{\Omega} \rho\gamma \mathrm{v}^* \mathrm{dV} + \int_{\Omega} \sigma : \dot{\varepsilon}^* \mathrm{dV} - \int_{\partial\Omega_c} \tau \mathrm{v}^* \mathrm{dS} = 0 \tag{1}$$

For almost steady-state processes, such as rolling, extrusion or wire drawing, an Euler description can be utilized where the domain Ω is considered as fixed. In this case, the major problem is to determine the free surface and to take into account memory effects, e. g. work hardening, for computing the stress tensor field.

In most non-stationary metal forming applications the inertia contribution can be neglected in equation (1) and an updated lagrangian approach is preferred, which corresponds to a first order integration scheme for the domain, the stress tensor and memory variables. On the domain Ω^t at time t equation (1) is approximated by:

$$\int_{\Omega^t} \sigma^{t+\Delta t} : \dot{\varepsilon}^* \mathrm{dV} - \int_{\partial\Omega_c^t} \tau^{t+\Delta t} \mathrm{v}^* \mathrm{dS} = 0 \tag{2}$$

Material points, stress tensor and memory variables (here the equivalent strain $\bar{\varepsilon}$) are updated according to:

$$\begin{aligned} x^{t+\Delta t} &= x^t + \Delta t v^t \\ \sigma^{t+\Delta t} &= \sigma^t + \Delta t \dot{\sigma}^t \\ \bar{\varepsilon}^{t+\Delta t} &= \bar{\varepsilon}^t + \Delta t \dot{\bar{\varepsilon}}^t \end{aligned} \tag{3}$$

The ALE (Arbitrary Lagrange Euler) formulation can be utilized when the boundary of the domain varies slowly, for example in ring rolling. A numerical velocity field v_{ALE} is defined in the domain, which is different from the material velocity. The material derivative for any variable is replaced by the ALE derivative, for example for $\bar{\varepsilon}$ we have:

$$\frac{d_{ALE}\bar{\varepsilon}}{dt} = \dot{\bar{\varepsilon}} + (v - v_{ALE}) grad(\bar{\varepsilon}) \tag{4}$$

The conservation of the boundary surface is imposed by following the condition on the normal vector *n:*

$$(v - v_{ALE}).n = 0 \tag{5}$$

2.2. Constitutive modeling

The first approaches of FE modeling of forming processes were based on a viscoplastic or rigid plastic behavior. In order to be able to model also the elastic component of the deformation, and more specifically to predict the residual stresses, an elastic viscoplastic or elastoplastic approach is selected where the strain rate is decomposed into an elastic part $\dot{\varepsilon}^e$ and an irreversible contribution $\dot{\varepsilon}^p$:

$$\dot{\varepsilon} = \dot{\varepsilon}^e + \dot{\varepsilon}^p \tag{6}$$

The elastic law is written with the Jauman derivative for material objectivity:

$$\frac{d_J \sigma}{dt} = \lambda \mathrm{tr}(\dot{\varepsilon}^e) + 2\mu \dot{\varepsilon}^e \tag{7}$$

Where λ and μ are the usual the Lamé coefficients. The viscoplastic contribution is often expressed by an isotropic Norton power law of the form:

$$\dot{\varepsilon}^p = 1/K \left\langle (\bar{\sigma} - R)/K \right\rangle^{\frac{1}{m}-1} \sigma' \tag{8}$$

We have introduced σ' the deviatoric stress tensor, $\bar{\sigma}$ the usual equivalent stress, *K* the material consistency and *m* the strain rate sensitivity.
More complicated constitutive equations are utilized to take into account anisotropy according to Hill or Barlat theories, or porous materials.

2.3. Contact, friction and wear

Contact occurs between the work-piece and the tools, between different parts of the tools or in the case of multi materials forming. For two bodies with velocities v_a and v_b the non-penetration condition is expressed as:

$$(v_a - v_b).n = \Delta v.n \leq 0 \tag{9}$$

Relative sliding between the two bodies generates a tangential friction stress τ_f at the interface $\partial\Omega_c$, that can be given for example by a Coulomb-Norton law:

$$\tau_f = -\mu_f(\sigma_n)\Delta v / |\Delta v|^{1-p_f} \tag{10}$$

Where μ_f is a function of the normal stress component σ_n and p_f is a friction coefficient.

Wear is a complicated physical phenomenon, the abrasion contribution depends on the normal stress, the relative velocity and the hardness of the tool H_V . It is often represented by a generalization of the Archard law:

$$\delta_W = K_W \cdot \int \frac{\sigma_n \cdot \Delta V}{{H_V}^{m_W}} \cdot dt \tag{11}$$

Where δ_W is the amount of wear, K_W and m_W are physical parameters associated with the material.

2.4. *Damage*

Fracture prediction during materials forming processes has been of utmost interest in the scientific and engineering community in the past century. Indeed, understanding and modeling ductile damage mechanisms remains a major issue to get defect-free products. Many phenomenological and micromechanical models were developed during the last twenty years to predict ductile fracture. These models are usually validated for given loading path (most of the time under monotonic loading) and specific materials, and their ability to be extended to other configurations – in terms of loading and materials – is often questionable. Enhancing these models is necessary for their application to real industrial processes. This requires accounting for non-proportional loadings (Bouchard et al., Gachet et al.) and for low stress triaxiality ratios. Recent studies also showed the influence of the third invariant of the deviatoric stress regarding ductile fracture critical strain. The Lode parameter was introduced by many authors in classical ductile damage models to get a better prediction of the influence of the stress state on ductile fracture (Nahshon and Hutchinson, Cao et al.). New mathematical formulations and numerical solution strategies dedicated to efficient modeling of continuum ductile damage and its transition to discontinuous fracture are also important. The use of non-local formulation coupled with anisotropic mesh adaptation is an efficient way to predict failure accurately and to model the transition between continuous damage approaches to discontinuous fracture (El Khaoulani and Bouchard). In the future, modeling of ductile failure at the micro scale appears to be essential to get a better understanding of microstructural heterogeneities for complex loading paths. Such microstructural simulations require being able to mesh complex microstructures and to model nucleation, growth and coalescence mechanisms for large plastic strain and complex loading paths. A new approach based on level set functions and anisotropic mesh adaptation is presented in section 7.

2.5. *Heat equation*

The classical integral form of the heat equation is written:

$$\int_{\Omega^t} \rho c\dot{T} w dV + \int_{\Omega^t} k\,grad(T)\,grad(w) dV - \int_{\Omega^t} \dot{q}_V w dV + \int_{\Omega^t} \phi_n w dS = 0 \tag{12}$$

Where w is a scalar test function, k is the thermal conductivity, $\dot{q}_V$ is the heat dissipated by plastic or viscoplastic deformation, ϕ_n is the heat flow on the boundary $\partial\Omega$, which comes from conduction, friction or radiation.

3. Space and time discretization

3.1 Tetrahedral elements

In metal forming simulation by the Finite Element method (FEM), the mesh is often progressively distorted and the resulting accuracy decreased so that the mesh must be regenerated periodically. Therefore the work-piece must be discretized by elements which are convenient for initial meshing and *automatic remeshing*. Tetrahedral elements are recognized as the most suitable for meshing and adaptive remeshing but, in order to avoid numerical locking, a mixed formulation must be used in term of displacement increment Δu (or velocity v) and pressure p. Neglecting inertia forces for an elastic plastic material, for any virtual displacement Δu^* and pressure p^*, we get:

$$\int_{\Omega} (\sigma' + \Delta\sigma') : \Delta\varepsilon^* dV - \int_{\Omega} p\,div(\Delta u^*) dV + \int_{\partial\Omega_c} \tau_f \Delta u^* dS = 0 \tag{13}$$

$$\int_{\Omega} \left(-div(\Delta u) - \frac{\Delta p}{\kappa} + 3\alpha_T \Delta T\right) p^* dV = 0 \tag{14}$$

Where κ is the compressibility coefficient and α_T is the linear dilatation coefficient. Pressure and temperature fields are discretized using tetrahedral elements with linear shape functions N_n, and a bubble function N_b is added to the displacement field (or the velocity field), in order to stabilize the solution for incompressible flow.

Introducing the nodal increment of displacement ΔU, the pressure increment ΔP and the temperature increment ΔT, we obtain a system of non-linear equations in the form:

$$R^U(\Delta U, \Delta P, \Delta T) = 0 \tag{15}$$

$$R^P(\Delta U, \Delta P, \Delta T) = 0 \tag{16}$$

$$R^T(\Delta U, \Delta P, \Delta T) = 0 \tag{17}$$

3.2 Time discretization

The classical formulation is based on a first order time integration scheme with the displacement and pressure increment. An implicit two order scheme based on a velocity approach was proposed for a viscoplastic behavior by Bohatier and Chenot and extended to elastic plastic materials by Chenot.
Another approach was developed by Mole et al in which the quasi static integral equation is differentiated with respect to time. A linear equation is obtained, which is easily solved in term of the acceleration nodal vector, while velocity and displacement fields are obtained by usual time integration method.
A simpler approach is to introduce an explicit Runge and Kutta integration scheme as it is presented in Traore et al for improvement of the accuracy in ring rolling, where the number of time increments must be very large.

3.3 Space-time finite element

The space-time finite element method has received a noticeable attention since 1969, in various fields including elastodynamics, where the boundary of the domain is subjected to small deformations. But there are few contributions in the field of metal forming which exhibits large or very large deformations. The potential advantage of space-time finite elements is the possibility of variable time increments on the space location (Fig. 1).

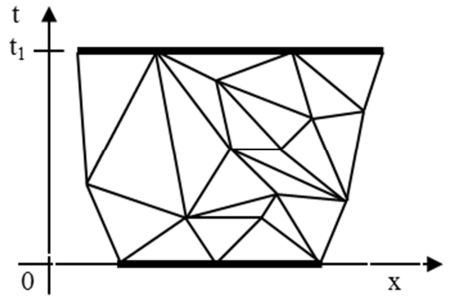

Fig. 1: Space time discretization for a simple 1-D problem.

Moreover error estimation can be extended to space-time in order to refine the mesh adaptively, not only in locations where elements are distorted with a uniform time increment, but also to generate more elements in the time dimension with fast evolution. This approach would involve a number of numerical developments, especially for meshing and remeshing 4-dimensional domain in space and time.

3.4 Remeshing and adaptive remeshing

For a more reliable control of accuracy, an estimation of the finite element discretization error is performed and the elements must be refined locally in the zones where the strain is higher. This is achieved by prescribing a local size of the elements and imposing that the mesh is rebuilt accordingly (Fourment and Chenot).

3.5 Anisotropic remeshing

Instead of utilizing regular tetrahedra and generate a very large number of elements we prefer to build anisotropic meshes having narrow elements in the direction of high strain gradient and elongated in the orthogonal direction (Gruau and Coupez). For that purpose a local metric matrix is defined in the local principal axes according to:

$$M = \begin{bmatrix} 1/h_1^2 & 0 & 0 \\ 0 & 1/h_2^2 & 0 \\ 0 & 0 & 1/h_3^2 \end{bmatrix} \tag{18}$$

Where h_1, h_2, h_3 are the thicknesses in the directions of principle axis of the tetrahedra to be generated locally.
In practice the metric tensor is composed of several contributions.
First the element should be refined in the direction of maximum gradient of the function, for example according to the strains rate tensor, we obtain the first contribution M^e to the metric.
Second, when thin parts are considered a "skin adaptation" is introduced in order to define the size h_s of the mesh in the thickness; the corresponding metric is:

$$M^s = \frac{1}{h_s^2} n \otimes n \rightarrow \begin{bmatrix} 1/h_s^2 & 0 & 0 \\ 0 & 0 & 0 \\ 0 & 0 & 0 \end{bmatrix} \text{ axis } n,\ t_1, t_2 \tag{19}$$

Where n is the normal to the surface and t_1, t_2 are any orthogonal tangential unit vectors.
Third to take into account local curvature of the boundary of the part, defined by the radii R_1 and R_2, a new contribution to the metric is given by:

$$M^c = \frac{1}{\alpha^2} \begin{bmatrix} 0 & 0 & 0 \\ 0 & 1/R_1^2 & 0 \\ 0 & 0 & 1/R_2^2 \end{bmatrix} \text{ axis } n,\ t_1, t_2 \tag{20}$$

The coefficient α is chosen in order to impose a minimum condition of angle variation on an element.
Finally the metric tensor is the sum of the three previous contributions:

$$M = M^e + M^s + M^c \tag{21}$$

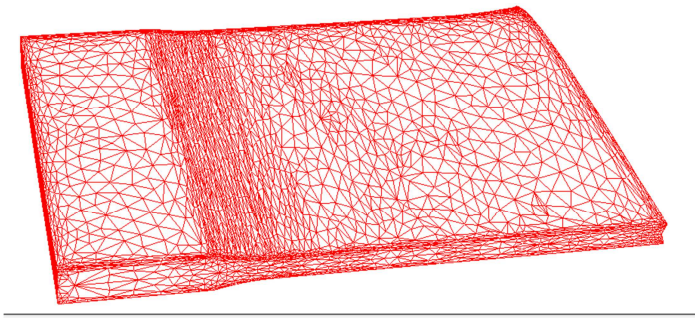

Fig. 2: anisotropic mesh for rolling

In order to generate an anisotropic mesh, a similar methods is used as for the isotropic previous isotropic remeshing procedure, but the distances are evaluated with the local metric tensor. This procedure can be applied to a large variety of processes. In Fig. 2 a simulation of rolling is made with an anisotropic mesh of 8 786 nodes which gives the same accuracy as the computation with an isotropic computation involving 61 474 nodes.

4. Resolution procedures

4.1 Linearization of the equations

The set of non-linear mechanical equations can be linearized using the classical Newton-Raphson method. We put $z=(\Delta u,\Delta p)$ and $R(z)=0$ for the two equations (15) and (16). Starting from a guess solution z^0 an iterative scheme is used to find the solution. At step number n, an increment δz^n to the current solution z^{n-1} is soughed so that: $R(z^n)=R(z^{n-1}+\delta z^n)=0$. After differentiation it is rewritten with the approximate form:

$$R(z^{n-1})+\frac{\partial R(z^{n-1})}{\partial z}\delta z^n=0 \tag{22}$$

We observe that we have to solve a series of linear systems for each time increment. This process can be shortened by optimization in the direction of δz^n , which means that we minimize with respect to β the residual:

$$\left\| R(z^{n-1}+\beta\delta z^n) \right\|^2 \tag{23}$$

When complex constitutive laws are involved, a modified Newton-Raphson method can be utilized. In this case the evaluation of the derivatives of the residual can be greatly simplified by numerical differentiation, but at the expense of extra computations.

4.2 Localized contact with the tools

Tools are considered as rigid, and their surfaces are discretized by triangular facets. The signed distance $\delta(M)$ between any point M of the domain and the tool is positive if the point is outside the tool, equal to zero if it is on the tool surface and negative if it has penetrated into the tool. A nodal contact approach (node-to-facet) is followed. For any node n, the contact condition is prescribed at the end of the time increment:

$$0\le\delta\left(M_n^{t+\Delta t}\right) \tag{24}$$

This equation is linearized with the assumption that the tool can locally be approximated by its tangential plane, which will be later referred to as an explicit scheme:

$$\delta_n^{t+\Delta t}=\delta(M_n^{t+\Delta t})\approx\delta(M_n^t)+\frac{d\delta}{dt}\left(M_n^t\right)\Delta t+O\left(\Delta t^2\right)\approx\delta_n^t+\left(v_{tool}^t-V_n^t\right).n_n^t\Delta t \tag{25}$$

Where v_{tool}^t is the tool velocity and n_n^t is the surface normal vector at the point of the tool surface which is the closest to node n. Contact equation (25) is enforced by a penalty formulation, which comes down at each time step t to minimizing a contact potential:

$$\varphi_{contact}(V)=\frac{1}{2}\rho\sum_{n\in\partial\Omega_c}\left[\left(V_n-v_{tool}\right).n_n-\left(\frac{\delta_n+\delta_{pen}^-}{\Delta t}\right)\right]^{+2}S_n \tag{26}$$

where ρ is a penalty coefficient, S_n is a surface portion associated to node n and δ_{pen}^{-} is a small numerical coefficient. This explicit formulation is accurate enough for many forming processes, but it sometimes results into numerical oscillations with important stresses or unjustified loss of contact with coarse meshes and an implicit algorithm has then to be preferred (Mahajan et al.) (Fourment et al.). The local plane approximation of the contact surface is updated at each new Newton-Raphson iteration, rather than at the end of time increment. It allows us to take into account possible evolutions of this surface during the time step Δt. The contact condition is then written as

$$\delta_i^{t+\Delta t} \approx \delta_{i-1}^{t+\Delta t} - \Delta v_i^{t+\Delta t}.n_{i-1}^{t+\Delta t}\Delta t \tag{27}$$

Where i is the i[th] Newton-Raphson iteration, $\Delta v_i^{t+\Delta t}$ is the Newton-Raphson velocity correction at iteration i, $n_{i-1}^{t+\Delta t}$ the normal of the tool surface at the projection of current node $x_{i-1}^{t+\Delta t}$, that is updated as follows:

$$x_i^{t+\Delta t} = x^t + v_i^{t+\Delta t}\Delta t = x_{i-1}^t + v_i^{t+\Delta t} \tag{28}$$

Contact algorithm can be improved by an approach based on higher order quadratic interpolation of the tools surface (Nagata) combined with a normal voting strategy (Page et al.). The resulting 3D contact algorithm provides smoother contact constraints along the discretized obstacle and increases simulation accuracy, especially in the case of metal forming processes with reduced contact area. With an explicit contact scheme, the additional computational cost is only few percent of the total computational time. With an implicit contact scheme, the continuity of the normal vectors also improves the algorithm convergence and consequently decreases its computational time.

4.3 Parallel computing

The power of computing is increasing rapidly, more than doubling every two years. It is anticipated, that in 2020, the supercomputers will have a performance of around 1 EFlops while desktop systems will obtain a performance of up to 100 TFlops. This context imposes also significant changes on our codes and the development of fully parallel platforms to take advantage of such increases in computer processing power (Coupez et al., Mesri et al.). We propose in our work a massively parallel methodology combined with mesh adaptation. Although the question of mesh adaptation has been addressed in the previous sections 3.4 and 3.5, we intend to retackle it, taking into account the current evolution of the parallel architecture, and the increase of computer powers, especially in terms of number of cores per processor.

Large scale parallel simulations involve meshes with millions to billions elements. With the increase of the latter, an interesting enhancement would be to deal with the mesh generation and adaptation in parallel. The parallelism of the mesh generator is performed here by partitioning/repartitioning the initial mesh into sub-meshes that are subsequently refined/unrefined according to the computed metric by using sequential procedure. The interfaces between subdomains remain unchanged during the local remeshing step, but are then moved along the domain to enable the remeshing in the following phases (Fig. 3). In other words, a repartitioning phase is performed to get unmeshed parts, those that were not yet processed, aggregated into the existing sub-domains. This partitioning/repartitioning of a mesh is performed in parallel using a generic graph partitioning that has been customized for FEM methods.

The proposed strategy of parallelization leads to several iterations (depending of the space dimension) between the mesher and the repartitioner, but the work to be done at each iteration decreases quickly. Indeed, an optimization method, based on a permute-copy-past algorithm, reduces the complexity from N (the data size) to m (the moving size) with m << N. It simply avoids having heavy copies of the entire data, instead it will apply permutations to the areas that need to be updated, perform the needed processing on these areas and then paste the processes area back

to where they belong. This optimization was essential to obtain a costless strategy with a high parallel pay-off of the mesher.

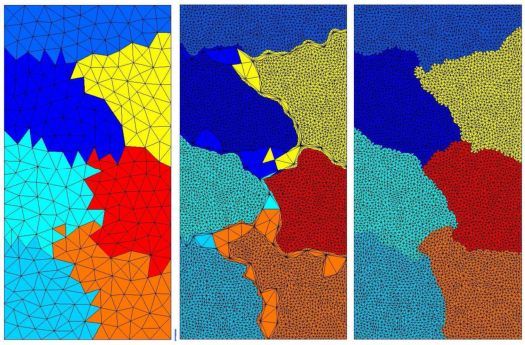

Fig. 3: Illustration of the parallelism strategy using a 2d test case on 7 processors (from left to right)

Finally, the parallel efficiency was tested using a soft scalability test from 8 to 8192 cores. Table 1 shows the results for the resolution of the incompressible Stokes equations using a mixed P1+/P1 finite element formulation. The loading of each core is around 420000 mesh nodes (representing 1260000 unknowns per core). The results in Table 1 show an almost constant time for solving the linear system that confirms the linear complexity of the algorithm but also a quasi-optimal use of all the cores as well as the memory. For thousands of cores, we have noticed an increase in the resolution time, but this is due to the strict imposed convergence rate on the coarse level grid (10^{-7}). The global system, contains more than 10 billion nodes, is solved using 8192 cores with 8 levels multigrid in 148 seconds consuming a total of 17,5Po of memory.

# cores	Assembling (s)	Resolution (s)	# Iterations	Memory (GB)
8	9.732	90.71	13	1.938
32	9.608	82.97	12	1.951
128	9.761	91.32	13	1.955
512	9.967	86.53	12	2.000
2048	10.60	93.7	12	2.077
8192	11.00	148.1	11	2.142

Table 1: Soft scalability test case using 8 to 8192 cores on GENCI (Grand Equipement National de Calcul Intensif)

4.4 Multi mesh

Incremental forging simulations are still challenging due to the required number of time steps to properly describe the process. As the deformation is often confined in a localized area, the temptation is to use specific mesh boxes to refine the mesh only in such area and use coarse meshes elsewhere to speed up the simulation. But, with such a technique, when the deformation area moves and the mesh is coarsened, most of the benefit of using a fine mesh is lost as the stress/strain distribution has to be remapped from a fine grid to a coarse one. Even without drastic coarsening it generates unacceptable diffusion due to cumulated remapping errors.

The first application of the bi-mesh technique was introduced by Kim et al. for ring rolling, and more recently for cogging by Hirt et al., or with a parallel implementation by Ramadan et al. The main idea is to separate the mesh devoted to the mechanical computation, called mechanical mesh (MM) in the following, from the mesh devoted to the thermal computation and to the storage of the results, called thermal mesh (TM). The user inputs a homogeneous fine thermal mesh and the software automatically derives an adapted mechanical mesh by systematic coarsening where it is allowed. The mechanical solution is computed on the adapted mesh and extrapolated on the fine mesh. As no deformation takes place in the de-refined area, extrapolation of the solution does not create any

significant error. From this solution, regular updating marching scheme algorithm may be applied to update mesh geometry and associated results (strain, stress, etc.) as well. Since the thermal problem is non-local, thermal equations are solved on the fine mesh.

We summarize in Figure 4 (a), the main steps of the bi-mesh algorithm. As we can see the standard single mesh algorithm (marked with white background) has been only slightly enriched by few specific steps (marked with a grey background).

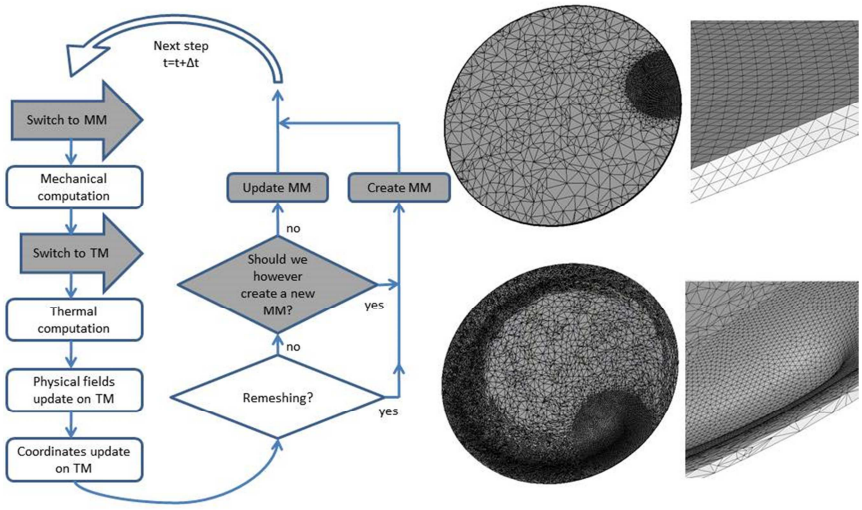

(a) (b)

Fig. 4: (a) General description of the bi-mesh algorithm, only the steps in grey background are specific to the bi-mesh method. (b) Examples of derived mechanical meshes from an homogeneous thermal mesh.

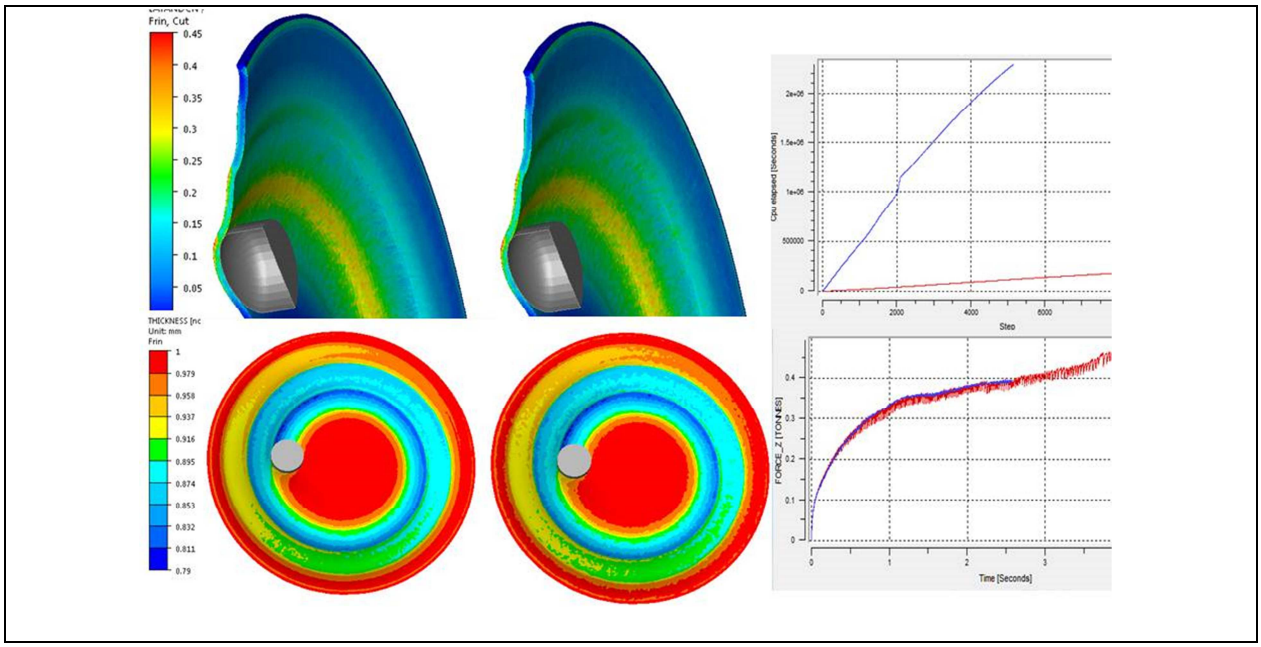

(a) (b) (c)

Fig. 5**:** Latham & Cockroft coefficients (up) and thickness (down). (a) With bi-mesh method (b) Without bi-mesh method. (c) CPU time (up) and vertical force on the punch (down) with bi-mesh (red lines) and without bi-mesh (blue lines).

4.5 Remapping

Transferring data between meshes is often a necessity in metal forming applications, as for instance in the multi-mesh approach and in the ALE (Arbitrary Lagrangian or Eulerian) formulation where this operation is involved at each time step, or in the Lagragian formulation where it is appealed to at each remeshing step. The precision of this operator is obviously a key issue for the overall accuracy of the finite element method, which so requires a special attention. In general, transferred fields can be split into two categories: primary unknowns of the problems such as velocity, pressure and temperature, and state variables such as the equivalent strain, strain rate and stresses. Firsts are usually continuous while seconds are computed at Gauss integration points and are discontinuous. With a P1+P1 velocity / pressure interpolation, they respectively are P1 (linear) and P0 (piecewise per element). Transferring data between non matching meshes involves diffusion error; it is all the more important than the field is discontinuous. It is so foremost important to develop high order operators for P0 variables but as they can be appealed to at each time increment, they should be inexpensive. The key idea of the developed approach is in two steps: computing a continuous high order (P1) interpolation of state variables on the original mesh and then projecting it on the Gauss point of the new mesh. Inherent diffusion of projection is compensated by higher order of the recovered field that is derived from super convergent properties of the finite element method at Gauss points. This approach has initially been proposed by Zienkiewicz and Zhu within the frame of error estimation (Superconvergent Patch Recovery method - SPR) before been extended to transfer operators by Khoei and Gharehbaghi. Considering finite element patches (see Fig. 6) a local higher order continuous solution is built from super convergent values. Its value at the patch center is then used to interpolate continuously (P1) the recovered field over the original mesh. This approach is shown to be significantly more accurate than simple local averaging or than global L^2 projection. However, it does not provide the same level of accuracy on the surface of the mesh where finite element patches are incomplete, while most important phenomena such as contact, friction and heat exchange take place on domain surface in metal forming applications. This would require enlarging the size of finite element patch (see Fig. 6), which necessitates a complex data structure that is often difficult to build in a parallel environment. Kumar et al developed an iterative algorithm, where complete volume patches are first recovered, and during next iterations, incomplete patches are enriched by new values recently computed at the nodes of the patch. Such algorithm converges within 3 to 4 iterations. For transferring complex analytical functions between non-matching 3D meshes, this operator has a second order convergence rate while the simple averaging technique is only slightly more than first order; the convergence rate of the averaging operator is much lower with the surface norm while it is almost the same with the SPR operator (Fig. 7). For several metal forming problems involving computation of residual stresses, the enhancements brought by this transfer operator is determinant to eliminate numerical oscillations otherwise resulting from the transfer.

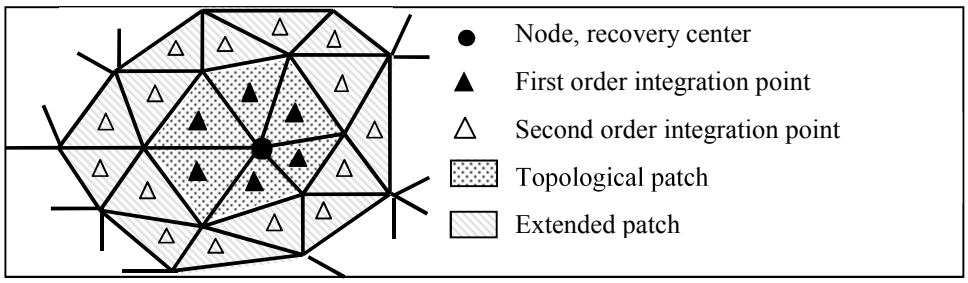

Fig. 6: Patch centre on a node in 2D

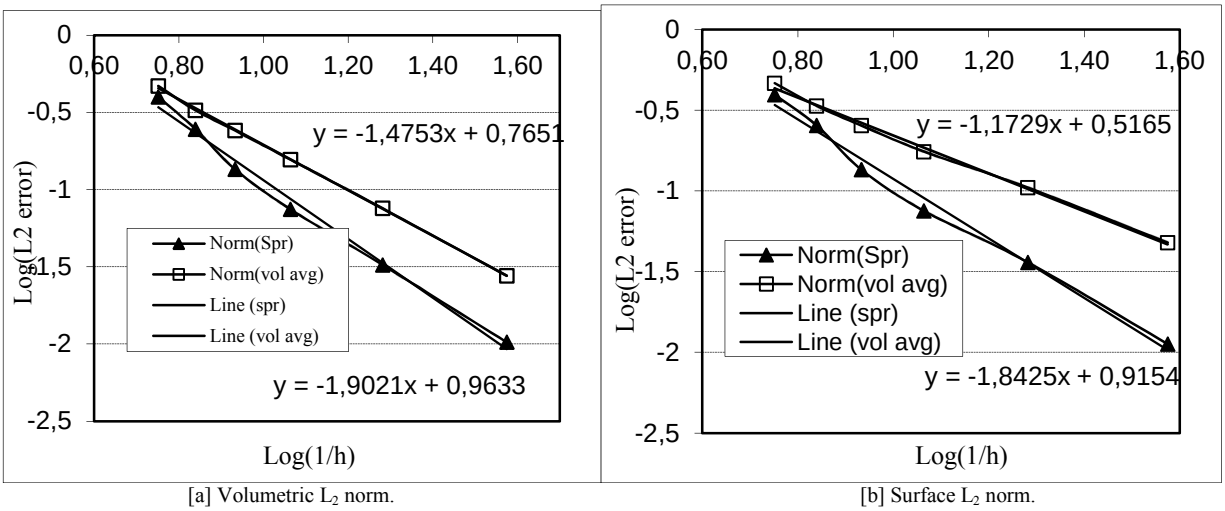

[a] Volumetric L_2 norm. [b] Surface L_2 norm.

Fig. 7: Comparison between SPR and Average recovery operator for function $f(x,y,z)=|z|(y-\beta|y|)sin(\alpha x)$

4.6 Multigrid

The constant need for more accuracy and reliability of computations results in smarter spatial discretizations and use of powerful parallel computers. Reducing the mesh size by a factor of 2 in each space direction results into an increase of the number of nodes by 8 (in 3D) and of the number of time increments by a factor 2. Because more than 75% of computational time of large implicit resolutions is spent during the resolution of linear systems, which computational cost is proportional to $N^{3/2}$ (N being the number of degrees of freedom), this increase in accuracy results into an increase of computational time by about 40. In order to handle larger and finer metal forming problems, it is then necessary to reduce the computational cost and more precisely the dependency of iterative solvers to the number of degrees of freedom, while keeping their parallel efficiency. According to Brandt, the Multigrid method (summarized in Fig. 8), which has originally been developed for fluid problems, has the unique potential of providing a linear computational cost with respect to N.

Function $MG(A_i, r_i)$
  if $i < n$ then
    $X_i \leftarrow S(A_i, b_i)$ // pre-smoothing step
    $r_i = b_i - A_i X_i$ // residual computation
    $r_{i+1} = R_i r_i$ // residual restriction
    $\delta X_{i+1} = MG(A_{i+1}, r_{i+1})$ // correction computation
    $\delta X_i = R_i^T \delta X_{i+1}$ // correction prolongation
    $X_i \leftarrow X_i + \delta X_i$ // correction
    $X_i \leftarrow S(A_i, b_i)$ // post-smoothing step
  else
    $X_i \leftarrow D(A_i, b_i)$ // coarsest grid direct resolution
  return X_i
end

Fig. 8: Multigrid V-cycle algorithm

For metal forming applications, obtaining such property requires using several special features for the choice of the smoothers (the linear solvers that are used at each level of the multi-level algorithm), for the construction of coarse levels using a Galerkin / algebraic approach rather than a geometrical approach, and for the automatic building of the coarse meshes (from finer unstructured meshes of very complex shapes as encountered in material forming): see Rey et al.. An additional issue regards the compatibility with parallel computations, which consequently requires carrying out all these operations in parallel, and more particularly the construction of coarse meshes (see Fig. 9) and the transfer between the meshes.

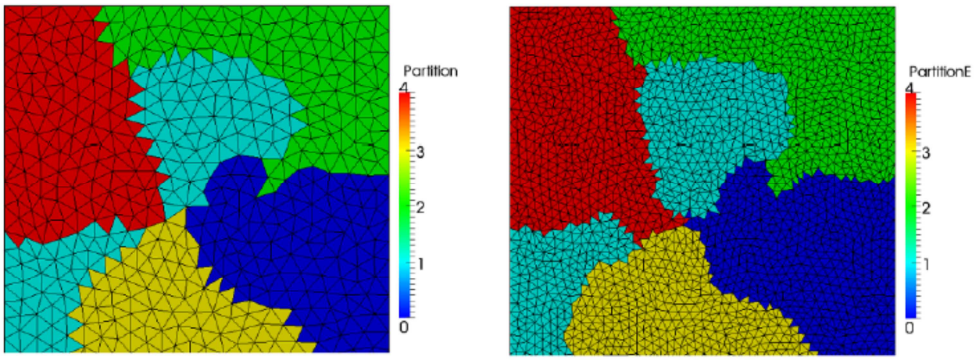

Fig. 9: Parallel partitioning of a square where different colors refer to different processors. Right: fine mesh. Left: coarse mesh built in parallel from fine mesh.

An application of the multigrid method to a representative forging problem is shown in Fig. 10. It is computed on a 12 processors machine where the multigrid solvers exhibits the same parallel efficiency as original Krylov solver.

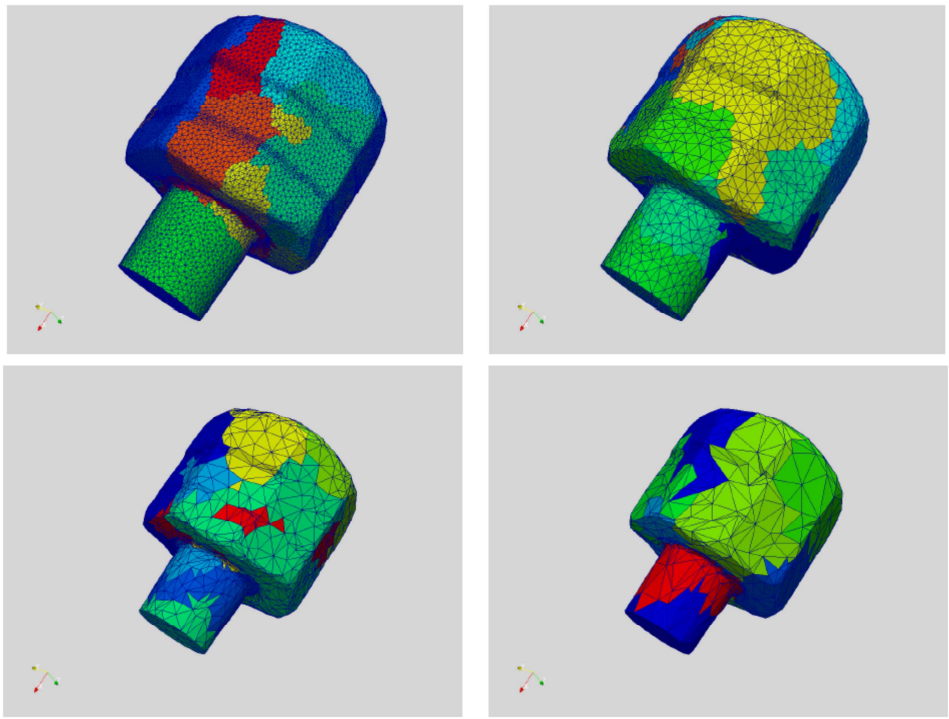

Fig. 10: Finer mesh (87 00 nodes) partitioned onto 12 processors for forging simulation (top left), and the intermediate meshes of 11 900 nodes, 3 800 nodes and 1 670 nodes for a four levels multigrid method.

5 Coupled approaches

5.1 Thermal and mechanical coupling

At this stage, several methods can be used, depending on the thermal and mechanical coupling. When coupling is weak enough, the mechanical and thermal problems are solved separately and the coupling is postponed to the next increment. For intermediate coupling a separate resolution is still used, but fixed point iterations are performed. For strong coupling and strain rate localization, the global system is solved by a Newton-Raphson method on V, P, and T (or ΔU, ΔP and ΔT) as reported in Delalondre.

5.2 Multi material coupling

Different numerical approaches are presented in paper 274 of the present ICTP conference by Chenot et al.

5.3 Coupling with micro structure evolution

Three approaches, working at different length scales, are used to predict the microstructural evolution during forming processes.
The classical semi-empirical JMAK approach is based on the global description of the recrystallized fraction in constant conditions of strain rate and temperature. Recrystallization kinetics (implying nucleation of new grains, their growth and the impingement of the growing grains) are described by the analytical Johnson-Mehl-Avrami-Kolmogorov (JMAK) equation.

$$X(t) = 1 - e^{-b.t^n} \tag{29}$$

Where X is the recrystallized fraction and b and n the Avrami's coefficients obtained by fitting the experimental curves. Dynamic, post-dynamic and static recrystallization can be considered; the different recrystallized fractions and diameters depend on the process parameters (strain, strain rate and temperature) and initial grain size. Implemented in the FORGE® software, the model has undergone several modifications in order to be used with any thermo-mechanical local loading and to take into account multiple recrystallization steps that can be encountered during multi-pass processes (see Teodorescu et al.).
The mean-field approach was developed in the general context of multi-pass metal processing. It uses equations based on the physics of strain-hardening, recovery, grain boundary migration, nucleation and precipitation. Input parameters have a physical meaning (e.g. Burgers vector, shear modulus, grain boundary mobility, etc.). The microstructure is described by a set of internal variables representative of the material (average dislocation densities and grain sizes). According to Mukherjee et al. and Bernard et al., the microstructural evolution is directly given by the evolution of these parameters during the forming process.

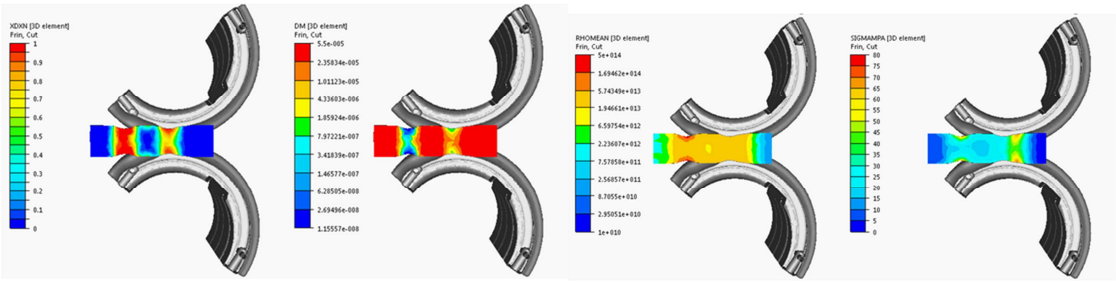

Fig. 11: Reducer-rolling simulation coupled with the mean-field model for microstructure evolution

Since the metal behavior depends on the dislocation density, such approach allows a direct coupling with the rheological behavior of the material. CPU times associated with these methods are generally low, making them suitable for coupled calculations and allowing simulations at each integration points of a finite element mesh as it is done into FORGE® (Fig. 11).

The full-field method is discussed in §7.

6 Optimization and identification

6.1 Process optimization

Optimization is often the actual purpose of numerical simulation. In metal forming, it usually involves a small number of parameters which can be quite complex as they often regard 3D tool shapes. Consequently, great efforts have been dedicated to the coupling of optimization algorithms with CAD tools, as shown in Fig. 12 where the parameters of the CAD representation of a preform shape are directly linked to the optimization algorithm.

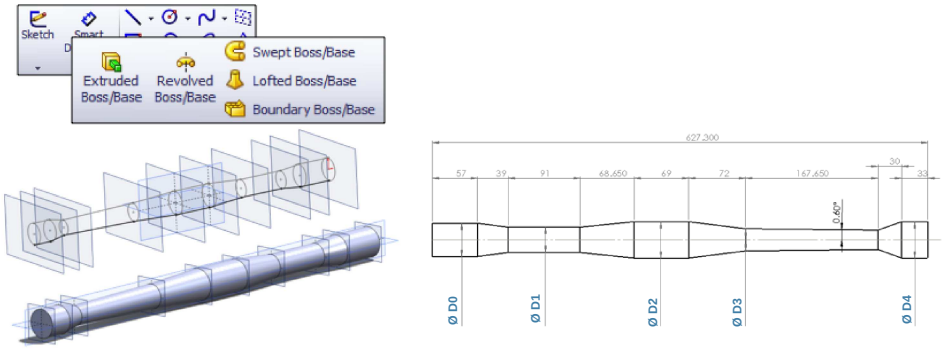

Fig. 12: CAD parameterization (left) of the preform shape of a three-stepped forged car component and its 4 optimization parameters.

Other features of metal forming problems regards the computational time of simulations and the complexity of the optimization problem, which can either be very small with almost linear problems or very high with many local extrema and uncertainties, resulting either from numerical noise (in particular due to remeshing and data transfer) or from the process model itself (friction, lubrication, material models …). All these features plead toward using robust but expensive algorithms, such as evolutionary algorithms, combined with metamodeling which allows reducing computational cost. A key point for the accuracy and efficiency of such metamodel based algorithm consists in dynamically improving the metamodel with new computations during the convergence of the optimization algorithm (see Bonte et al.). In this context, numerical noise can be handled by filtering the very high frequencies of objective functions through the smoothing of the metamodel as presented in Fig. 13. We observe that for a wire drawing problem, a straightforward variation of the maximum drawing force with respect to the die angle and die length shows an unphysical extremum due to numerical noise due to remeshing (with coarse meshes), while smoothing allows removing this biased solution. Metamodel-based evolution algorithms can easily be extended to multi-objective optimization problems, in order to handle the full complexity of most engineering problems with several objectives and constraints. In this frame, there is not a single optimum but a Pareto surface of possible compromises. The computational cost of optimization is consequently increased by the need to enlarge the domain of accuracy of the metamodel as shown by Edjay and Fourment. This additional cost is often justified by the quality of provided information and new understanding about the forming process.

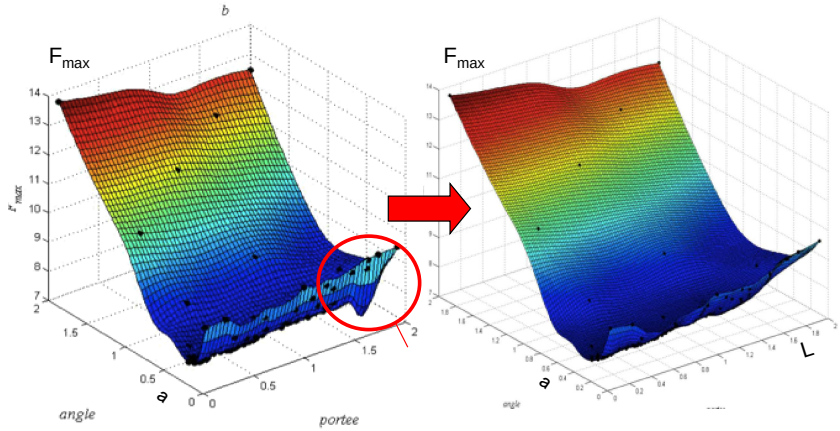

Fig. 13: Left: metamodel of the noisy objective function exhibiting an unphysical extremum. Right: smoothed metamodel with no extremum.

6.2 Identification of material parameters

Identifying correctly material parameters is essential if one wants to get accurate results with any kind of material behavior law and damage model. Identification strategies using inverse analysis are now widely used when dealing with complex non-linear behaviors. The main idea of inverse approaches is to fit numerical results coming from a FE simulation on experimental data. This fitting is done iteratively by tuning the material parameters values in the model in order to minimize a cost function. This cost function is based on the gap between numerical and experimental observables. The choice of these observables and their number is important if one wants to avoid any parameters correlation or non-unique solutions issues (Roux). This is particularly true when dealing with ductile damage due to the competition between hardening on the one hand and softening (coming both from necking and damage growth) on the other hand. The use of local observables in addition to global observables (such as the classical load-displacement curve) is a good way of enriching the cost function. Local observables may be based on necking measurements (Roux and Bouchard) or full displacement field measurements (Roux). Enhancing the experimental basis to avoid non-unique solutions may also require the use of multiple experimental tests (Cao et al. 2013). Finally, some micromechanical models may require the use of microstructure observations. Regarding ductile damage parameters identification, in-situ X-Ray tomography appears to be a powerful solution. This technique enables to count the number of voids and to give their size evolution all along the mechanical test. This approach was successfully used in (Cao et al. 2014b) for the identification of a Gurson based damage model.

7 Computation at the micro-scale

7.1 General approach

It is well known that the micro (or nano) structure of metals is a key factor for determining the constitutive law during forming and for predicting the final properties of the work-piece. The macro approach is quite convenient for coupling thermal, mechanical and physical computation, but it suffers severe limitations and needs a large amount of experiments to identify the physical laws describing microstructure evolution. On the other hand computation at the micro scale is now possible and is developed for a potentially more realistic description of materials under the concept of “full field approach”. Micro modeling is potentially much more accurate but, due to heavier computer cost at the local micro level, direct coupling with macro thermal and mechanical simulations seems limited to 2D problems and simple parts, even with large clusters of computers. If, as already detailed, one interest of these developments is to use the micro approach to help identification and improvement of mean field models; another way to view the short term applications is to use micro modeling of material in post processing, to predict micro structure evolution for a limited number of locations in the work piece, neglecting coupling effects.
These challenges explain firstly the development, over the last twenty years, of new numerical methods to generate digital materials at a microscopic or mesoscopic scale, which would be statistically or exactly equivalent to the considered microstructure in terms of topology and attributes and the concept of Representative Element Volume

(REV) (Dawson et al., Hitti et al., Saby et al. 2013). The generation of statistical virtual polycrystals in context of recrystallization (ReX), or of spheres dense packing applied to powder metallurgy, remain fertile research domains (see Fig. 14).

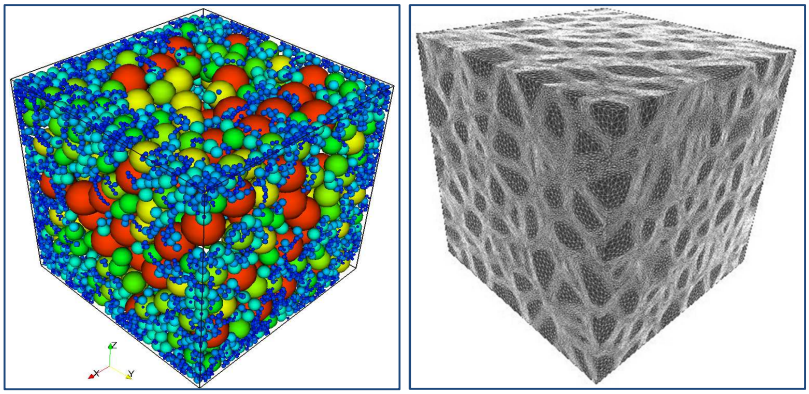

Fig. 14: REVs respecting initial statistical data. Left a 304L powder. Right: 304L polycrystal with anisotropic finite element mesh in white.

Secondly, these challenges explain the development of numerical methods dedicated to the modelling of dynamic boundary problems. Probabilistic methods associated to a voxel (or pixel in 2D) can be based on grain structure descriptions; for instance, Monte-Carlo (MC) (Rollett and Raabe) and Cellular Automaton (CA) approaches have been successfully applied to ReX, grain growth (GG) and phase transformations (Rollett and Raabe, Kugler and Turk).

Three main methods can be found in the literature for finite element calculations on virtual micro-structures: the "vertex" models (VM) also called "front tracking" models (Nagai et al., 1990, the "Phase Field" method (PFM) (Chen) and the "Level Set" method (LSM) first developed by Osher and Sethian.

The LSM was applied to dynamic interface problems at the microstructure scale for 2D or 3D primary ReX and includes site saturated or continuous nucleation stage as illustrated in Fig. 15 (Logé et al., Bernacki et al., 2008, Bernacki et al., 2009).

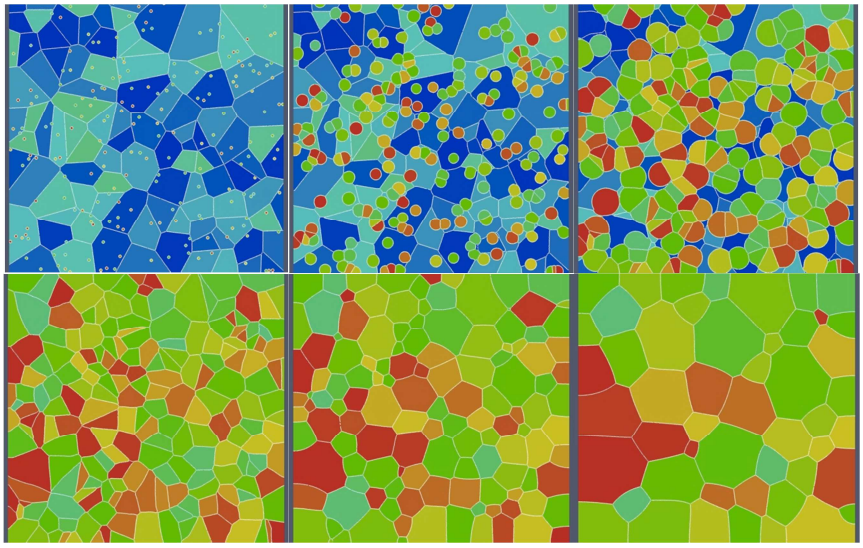

Fig. 15: Site-saturated nucleation in 304L stainless steel, from top to bottom and left to right : modeling of primary ReX and subsequent GG.

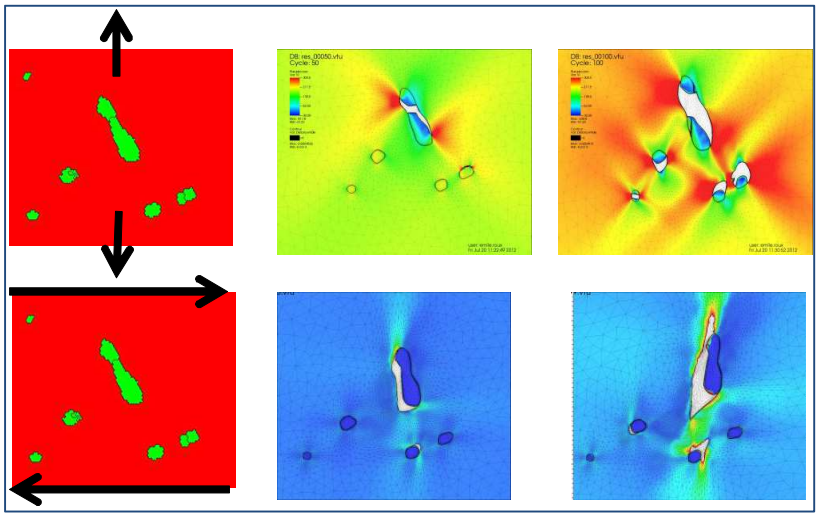

Fig. 16: Influence of loading conditions on nucleation mechanism (particles fracture or debonding).

First applied to simple microstructures, LSM was improved to deal with more realistic 2D and 3D microstructures and to make the link with stored energies induced by large plastic deformations (Logé et al., Bernacki et al., 2009). Anisotropic meshing and remeshing techniques can be used to accurately describe interfaces, both for modelling plastic deformation using crystal plasticity, and for updating the grain boundary network at the RX stage (Logé et al., Bernacki et al. 2009). It was also shown that the distribution of stored energy in a polycrystal resulting from plastic deformation led to deviations from the classical JMAK theory. Recently, for the modelling of ReX and GG phenomena, the LSM has been used in (Elsey et al.) with a regular grid and in (Bernacki et al, 2011) from a finite element approach. It is also interesting to underline current development of the LSM in order to model ductile damage phenomena at the micro scale as illustrated in Fig. 16 (Roux et al., 2013), (Roux et al., 2014).

7.2 *Identification using finite element micro modeling*

Such micro-modeling approaches are very promising regarding the understanding of plastic and damage mechanisms for complex thermo mechanical loadings as well as the calibration of mean field models.

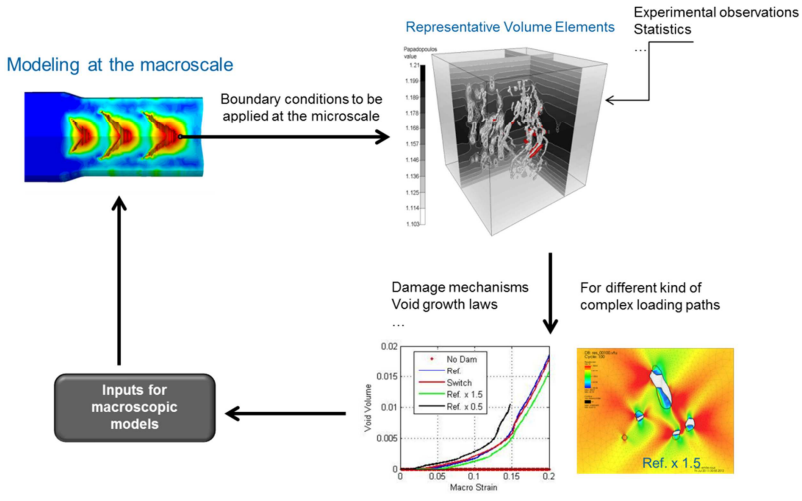

Fig. 17: Multiscale methodology to identify mean-field models parameters thanks to microscale FE simulations

Figure 17 shows the strategy that can be applied to identify mean-field models parameters based on micromechanical modeling. Numerical sensors are placed on finite element simulations of the process at the macro scale in order to extract loading paths. This loading path can be used as boundary conditions for FE simulations at the micro-scale on representative volume elements (RVE). These RVE are built either from experimental observations or from statistical reconstruction. FE simulations on these RVE with the appropriate boundary conditions are performed in order to extract microscopic evolution laws. In Fig. 17, void volume fraction as a function of plastic strain is plotted. These evolution laws are then used to identify mean-field damage models parameters which in the end will be used in macroscopic scale FE simulations. The same methodology is applied in (Saby et al. 2013, Saby et al. 2014a, Saby et al. 2014b) to define a suitable void closure criterion and identify its parameters.

8 Future challenges:

8.1 Process stability and introduction of stochastic phenomena

Provided that the problem is well modeled, numerical simulation is predictive and describes accurately all phenomena of interest. It means that the finite element discretization error is low and often much lower than errors resulting from the modeling of the problem. Taking into account the main sources of these uncertainties is a major challenge of computations. Uncertainties have many origins: changes of material origin, lubrication conditions or process parameters but also approximate modeling of interface and material behavior, or else geometry description, boundary conditions, etc. The challenge consists in first identifying, modeling and quantifying these uncertainties and then in taking them into account during process simulation and optimization (Strano). Monte-Carlo approaches are obviously too expensive while stochastic formulations show quite difficult to implement into existing software. Most promising approaches rely on advanced metamodels that can be either used for a Monte-Carlo type approach (Fourment) or extended to model the stochastic nature of the results (Zabaras et al., Lebon et al.) and can be both used to render process variability and allow robust optimization (Wienbenga et al).

8.2 Model reduction

Reducing computational time remains a major challenge. New emerging techniques show quite efficient and effective: the Proper Orthogonal Decomposition (PGD) method is one of them. It allows carrying out real time simulations, provided that pre-computations have been carried out in advance in a proper way (Chinesta and Cueto). In the frame of highly non-linear metal forming problems, a first step would be to extend Model Reduction Techniques resulting from Proper Orthogonal Decomposition (Ryckelynck). In some other fields such as fluid mechanics or structural mechanics, they allow reducing the computational time by several order of magnitude through a dramatic reduction of the number of unknowns, down to ten or at least less than one hundred. They are based on projections onto main problem modes, which are computed in advance from previous simulation results. It sounds reasonable to try to extend them first to simple metal forming problems.

8.3 Toward simulation of the whole processes chain

Forming process simulation started in the 70th with, as a main objective, to predict forming forces, forming defects such as under filling, folding and possible cracks. When this has been achieved, focus has started to move to the dies with the goal to predict and improve die life and reduce production costs. If there are still some progress to be done, stress distribution and die wear are now available in simulation packages. This second point being achieved, focus is back on the component with a specific attention to “in use properties”. These properties are the results of the whole manufacturing chain: starting with the initial forming process (rolling, cogging or wire drawing), going through the whole chain to ends with the final heat treatments (carburizing, quenching, nitriding, tempering). Depending on the situation, some of the “in use properties" are already available by simulation while others are still ahead. Significant progresses have been made in recent years and it is now possible to simulate and to optimize complete chains of simulations (Ducloux, Ducloux et al). The contributions of upstream stages such as ingot casting or continuous casting can also be taken into account and then allow to monitor the complete process chain with the prediction of porosities, segregations, concentrations of chemical elements during solidification to

their evolution during the phases of forging. It gives a better understanding of the internal structure of the forged part (Jaouen et al. 2014a) and for example can be an aid in the design of shells produced from hollow ring (Jaouen et al. 2014b).
For a better understanding of the “in use properties” a finer description of the micro structure is needed. It requires predicting and following the micro structure evolution through the whole process chain which is still a topic in progress and existing models stills need to be developed and improved in order to optimize computation time.

9 Conclusions

After many years of continuous development, simulation of metal forming processes by the finite element method has reached an undisputable level of reliability and is currently utilized in many industrial companies for predicting important technical parameters. Most of mechanical issues are treated satisfactorily, even if computational developments are still necessary to optimize numerical treatments and take into account new problems. Now within the next 10 or 20 years a lot of effort is necessary to model accurately the physical evolution of metallic materials during forming and heat treatments and to predict the final properties of work-pieces and assemblies.

References

[1] Bernacki M., Resk H., Coupez T., Logé R., 2009, Finite element model of primary recrystallization in polycrystalline aggregates using a level set framework, Simul. Mater. Sci. Eng., 17, 064006.
[2] Bernacki M., Loge R., Coupez T., 2011, Level set framework for the finite-element modelling of recrystallization and grain growth in polycrystalline materials, Scripta Mat. 64, 525-528
[3] Bernard P., Bag S., Huang K., Logé R. E., 2011, A two-site mean field model of discontinuous dynamic recrystallization, Materials Science and Engineering, A 528, 7357-7367
[4] Bohatier C, Chenot J.-L., 1985, Finite element formulations for non-steady-state large viscoplastic deformation, Int. J. for Numerical Methods in Engineering, 21, 9, 1697–1708
[5] Bonte M., Fourment L., Do T, van den Boogaard A., Huétink J., 2010, Optimization of forging processes using Finite Element simulations, Structural and Multidisciplinary Optimization, 42, 5, 797-810
[6] Bouchard P.-O., Bourgeon L., Fayolle S. Mocellin K., 2011, An enhanced Lemaitre model formulation for materials processing damage computation, Int. J. Mater. Form., 4(3), 299-315
[7] Brandt A., 2002, Multiscale Scientific Computation: Review 2001, in Multiscale and Multi resolution Methods, T. Barth, T. Chan, and R. Haimes Editors., Springer, Berlin, 3-95
[8] Cao T.S., Gaillac A., Montmitonnet P., Bouchard P.-O., 2013, Identification methodology and comparison of phenomenological ductile damage models via hybrid numerical-experimental analysis of fracture experiments conducted on a zirconium alloy, International Journal of Solids and Structures, 50, 24, 3989-3999
[9] Cao T.-S, Gachet. J.-M, Montmitonnet P., Bouchard P.-O., 2014, A Lode-dependent enhanced Lemaitre model for ductile fracture prediction at low stress triaxiality, Engineering Fracture Mechanic, 124–125: 80-96
[10] Cao T.S., Maire E., Verdu C., Bobadilla C., Lasne P., Montmitonnet P., Bouchard P.-O., 2014b, Characterization of ductile damage for a high carbon steel using 3D X-ray micro-tomography and mechanical tests - Application to the identification of a shear modified GTN model Computational Materials Science, 84, 175-187
[11] Chen L.Q., 1995, A novel computer simulation technique for modeling grain growth, Scr. Metall. Mater., 32, 1, 115-120
[12] Chenot J.-L., 1984, A velocity approach to finite element calculation of elastoplastic and viscoplastic deformation processes, Engineering Computations, 5, 1, 2 - 9
[13] Chenot J.-L., Béraudo C., Bernacki M., Fourment L., 2014, Finite Element simulation of multi material metal forming, 11th International Conference on Technology of Plasticity, ICTP 2014, 19-24 October, Nagoya, Japan
[14] Chinesta F., Cueto E., 2014, Introduction, in PGD-Based Modeling of Materials, Structures and Processes, Springer International Publishing, 1-24
[15] Cornfield G. C., Johnson R. H., 1973,Theoretical predictions of plastic flow in hot rolling including the effect of various temperature distributions, J. Iron Steel Inst., 211, 567
[16] Coupez T., Digonnet H., Ducloux R., 2000, Parallel meshing and remeshing, Applied Mathematical Modelling, 25, 153-157
[17] Dawson P.R., Miller M.P., Han T.-S., Bernier J., 2005, An Accelerated Methodology for the Evaluation of Critical Properties in Polyphase Alloys, Metal. Mater Trans A 36A , 7, 1627-1641
[18] F. Delalondre, 2008, Simulation and 3-D analysis of adiabatic shear bands in high speed metal forming processes, PhD Mines ParisTech, Sophia-Antipolis, 243 (in French)
[19] Ducloux R., 2013, From the forging to the complete manufacturing chain Simulation, 46th ICFG Plenary Meeting, Paris
[20] Ducloux R., Barbelet M., Fourment L., 2013, Automatic optimization of a complete manufacturing chain, NUMIFORM, AIP Conf. Proc. 1532, 665
[21] Ejday M., Fourment L., 2010, Metamodel assisted multi-objective optimization for metal forming applications, Mecanique & Industries, 11, 3-4, 223-233.
[22] El Khaoulani R., Bouchard P.-O., 2012, An anisotropic mesh adaptation strategy for damage and failure in ductile materials, Finite Elements in Analysis and Design, 59, 1-10

[23] Elsey M., Esedoglu S., Smereka P., 2009**,** Diffusion generated motion for grain growth in two and three dimensions, Journal of Computational Physics, 228, 21, 8015-8033.
[24] Fourment L. and Chenot J.-L., 1992, Computational Plasticity, Fundamentals and Applications, ed. by Owen D. R. J. et al., Pineridge Press, Swansea, U.K., 199-212
[25] Fourment L., 2007, Meta-model based optimisation algorithms for robust optimization of 3D forging sequences, in 10th ESAFORM Conference on Material Forming, Pts A and B, E. Cueto and F. Chinesta, Editors, 21-26
[26] Fourment, L., Chenot J. L., Mocellin K., 1999, Numerical formulations and algorithms for solving contact problems in metal forming simulation, International Journal for Numerical Methods in Engineering 46, 9, 1435-1462
[27] Gachet J.-M., Delattre G., Bouchard P.-O., 2014, Fracture mechanisms under monotonic and non-monotonic low Lode angle loading, Engineering Fracture Mechanics, 124–125, 121-141
[28] Gruau C., Coupez T., 2005, 3D tetrahedral, unstructured and anisotropic mesh generation with adaptation to natural and multidomain metric, Comp. Meth in Appl. Mech and Engrg, 194, 48-49, 4951-4976
[29] Hirt G., Kopp R., Hofmann O., Franzke M., Barton G., 2007, Implementing a high accuracy Multi-Mesh Method for incremental Bulk Metal Forming, CIRP Annals-Manufacturing Technology, 56, 313-316
[30] Hitti K., Laure P., Coupez T., Silva L., Bernacki M., 2012, Precise generation of complex statistical Representative Volume Elements (RVEs) in a finite element context, Computational Materials Science, 61, 224-238
[31] Iwata K., Osakada K., Fujino S., 1972, *Analysis of hydrostatic extrusion by the finite element method*., Transactions of the ASME, Ser. B, 94-2, 697-703
[32] Jaouen O., Costes F., Barbelet M., Lasne P., 2014a, From continuous casting to rolling process simulation with a full 3D powerful software tool,1st ESTAD & 31st JSI, 7-8 April, Paris
[33] Jaouen O., Costes F., Lasne P., Fourment C., Barbelet M., 2014b, Numerical simulation of a shell forming, from hollow ingot to the final product, with a powerful software tool, 2nd International Conference on Ingot Casting Rolling & Forging, ICRF2014, Milan, 7 to 9 May
[34] Khoei, A.R. , Gharehbaghi S.A., 2007, The superconvergence patch recovery technique and data transfer operators in 3D plasticity problems, Finite Elements in Analysis and Design, 43, 8, 630-648.
[35] Kim N., Machida S., Koboyashi S., 1990, Ring rolling process simulation by the three dimensional finite element method, Int. J. Machine Tools and Manufacture, 30, 569-577
[36] Kugler G., Turk R., Study of the influence of initial microstructure topology on the kinetics of static recrystallization using a cellular automata model, 2006, Comput. Mater. Sci., 37, 284-291
[37] Kumar S., Fourment L., Guerdoux S., 2014, Parallel, second-order and consistent remeshing transfer operators for evolving meshes with superconvergence property on surface and volume. Finite Elements in Analysis and Design, (submitted).
[38] Lebon J., Le Quillec G., Breitkopf P., Coelho R. F., Villon P., 2014, A two-pronged approach for springback variability assessment using sparse polynomial chaos expansion and multi-level simulations, International Journal of Material Forming,. 7, 3, 275-287
[39] Lee C. H., Kobayashi S., 1973, New Solutions to Rigid-Plastic Deformation Problems Using a Matrix Method, J. Eng. Ind., 95, 865
[40] Logé R., Bernacki M., Resk H., Delannay L., Digonnet H., Chastel Y., Coupez T., 2008, Linking plastic deformation to recrystallization in metals using digital microstructures, Phil. Mag., 88, 3691-3712
[41] Mahajan, P., Fourment L, Chenot J.-L., 1998, Implicit scheme for contact analysis in non-steady state forming, Engineering Computations, 15, 6-7, 908-924
[42] Mesri Y., Zerguine W., Digonnet H., Silva L., Coupez T., 2008, Dynamic parallel mesh adaption for three dimensional unstructured meshes: Application to interface tracking. Proceeding of the 18th IMR, Springer,195-212,
[43] Mole N., Chenot J. –L., Fourment L., 1996, A velocity based approach including acceleration to the finite element computation of viscoplastic problems, Int. J. Numer. Methods Engng., 39, 3439-51
[44] Mukherjee M., Prahl U., Bleck W., 2010, Modelling of microstructure and flow stress evolution during hot forging, Steel Research Int. 81, 1102-1116
[45] Nagai T., Ohta S., Kawasaki K., Okuzono T., 1990, Computer simulation of cellular pattern growth in two and three dimensions, Phase Trans., 28, 177-211
[46] Nagata, T., 2005, Simple local interpolation of surfaces using normal vectors, Computer Aided Geometric Design, 22,327–347
[47] Nahshon K., Hutchinson J., 2008, Modification of the Gurson model for shear failure, Eur. J. Mech. A/Solids, 27(1), 1–17
[48] Page D. L., Sun Y., Koschan A. F., Paik J., Abidi M. A., 2002, Normal Vector Voting: Crease Detection and Curvature Estimation on Large, Noisy Meshes, Graphical Models, 64, 199-229
[49] Ramadan M., Fourment L., Digonnet H., 2009, A parallel two mesh method for speeding-up progresses with localized deformations: application to cogging, Int. J. of Material Forming, 2, Supplement 1, 581-584
[50] Osher S. and Sethian J. A., 1988, Fronts propagating with curvature-dependent speed: Algorithms based on Hamilton-Jacobi formulations, J. Comp. Phys., 79, 12-49
[51] Rey B., Mocellin K., Fourment L., 2008, A node-nested Galerkin multigrid method for metal forging simulation. Computing and Visualization in Science, 11, 1, 17-25
[52] Rollett A. D., Raabe D., 2001, A hybrid model for mesoscopic simulation of recrystallization, Comput. Mater. Sci., 21, 69-78
[53] Roux E., 2011, Mechanical joining- Process optimization strategies and identification of materials mechanical behaviors , PhD at Ecole des Mines de Paris, Sophia Antipolis (in French)
[54] Roux E., Bouchard P.-O., 2011, Numerical investigation of ductile damage parameters identification: benefit of local measurements, ICIPE international conference, Orlando, Floride USA.
[55] Roux E., Bernacki M., Bouchard P.-O., 2013, A level-set and anisotropic adaptive remeshing strategy for the modeling of void growth under large plastic strain, Computational Materials Science, 68, 32-46
[56] Roux E., Shakoor M., Bernacki M., Bouchard P.-O., 2014, A new finite element approach for modelling ductile damage void nucleation and growth – analysis of loading path effect on damage mechanisms, accepted for publication in Modelling and Simulation in Materials Science and Engineering

[57] Ryckelynck D., 2009, Hyper-reduction of mechanical models involving internal variables, Int. J. Numer. Meth. Engng., 77, 1, 75-89
[58] Saby M., Bernacki M., Roux E., Bouchard P.-O., 2013, Three-dimensional analysis of real void closure at the meso-scale during hot metal forming processes, Computational Materials Science, 77, 194-201
[59] Saby M., Bernacki M., Bouchard P.-O., 2014a, Understanding and modeling of void closure mechanisms in hot metal forming processes: a multiscale approach, 11th International Conference on Technology of Plasticity, ICTP, 19-24 October 2014, Nagoya Congress Center, Nagoya, Japan
[60] Saby M., Bouchard P.-O. Bernacki M., 2014b, Void closure criteria for hot metal forming: a review, Journal of Manufacturing Processes (in Press)
[61] Strano M. A, 2008, Technique for FEM optimization under uncertainty of time-dependent process variables in sheet metal forming, Int. J. Mater. Form., 1, 13-20
[62] Surdon G., Chenot J.-L., 1987, Finite element calculation of three-dimensional hot forging, Int. J. Numer. Meth. Eng., 24, 2107-2117
[63] Teodorescu M., Lasne P., Logé R., 2007, Modeling recrystallization for 3D multi-pass forming processes, Materials Science Forum, 558-559, 1201-1206
[64] Traore K., Forestier R., Mocellin K., Montmitonnet P., Souchet M., 2001, Three dimensional finite element simulation of ring rolling, 7th International Conference on Numerical Methods in Industrial Forming Processes NUMIFORM 2001, Toyohashi, Japan
[65] Wagoner R. H., Chenot J.-L., 2001, *Metal forming analysis*, Cambridge, Cambridge University Press
[66] Wiebenga J. H., Weiss M., Rolfe B., Van Den Boogaard A. H., 2013, Product defect compensation by robust optimization of a cold roll forming process, Journal of Materials Processing Technology, 213, 6, 978-986
[67] Zabaras N., Bao Y., Srikanth A., Frazier W. G., 2000, A continuum Lagrangian sensitivity analysis for metal forming processes with applications to die design problems, Int. J. Numer. Meth. Engng, 48, 679–720
[68] Zienkiewicz O. C., Godbole K., 1974, Flow of Plastic and Visco-Plastic Solids with Special Reference to Extrusion and Forming Processes, Int. J. Numer. Meth. Eng., 8, 1, 1-16
[69] Zienkiewicz, O.C., Zhu J.Z., 1992, The superconvergent patch recovery (SPR) and adaptive finite element refinement, Computer Methods in Applied Mechanics and Engineering, 101, 207-224